Experimental investigation and theoretical analysis of a nonlinear energy sink under harmonic forcing

Etienne Gourc, Guilhem Michon, Sébastien Seguy, Alain Berlioz

Proceedings of the ASME 2011 International Design Engineering Technical Conferences & Computers and Information in Engineering Conference
IDETC/CIE 2011
August 28-31, 2011, Washington, DC, USA

DETC2011/VIB-48090

DRAFT: EXPERIMENTAL INVESTIGATION AND THEORETICAL ANALYSIS OF A NONLINEAR ENERGY SINK UNDER HARMONIC FORCING

Etienne Gourc*
Université de Toulouse, INSA
ICA (Institut Clément Ader)
F-31077, Toulouse, FRANCE

Guilhem Michon
Université de Toulouse, ISAE
ICA (Institut Clément Ader)
F-31055, Toulouse, FRANCE

Sébastien Seguy
Université de Toulouse, INSA
ICA (Institut Clément Ader)
F-31077, Toulouse, FRANCE

Alain Berlioz
Université de Toulouse, UPS
ICA (Institut Clément Ader)
F-31062, Toulouse, FRANCE

ABSTRACT

In the present works, we examine experimentally and theoretically the dynamic behavior of linear oscillator strongly coupled to a nonlinear energy sink under external periodic forcing. The nonlinear oscillator has a nonlinear restoring force realized geometrically with two linear springs that extend axially and are free to rotate. Hence, the force-displacement relationship is cubic. The linear oscillator is directly excited via an electrodynamic shaker. Experiments realized on the test bench consist of measuring the displacement of the oscillators while increasing and decreasing frequencies around the fundamental resonance of the linear oscillator. Many nonlinear dynamical phenomena are observed on the experimental setup such as jumps, bifurcation, and quasiperiodic regimes. The retained nonlinear model is a two degree of freedom system. The behavior of the system is then explained analytically and numerically. The complexification averaging technique is used to derive a set of modulation equation governing the evolution of the complex amplitude at the frequency of excitation, and a stability analysis is performed.

*Address all correspondence to this author: gourc@insa-toulouse.fr

INTRODUCTION

The most common vibration absorbtion system is the well known Tuned Mass Damper (TMD). However, the efficiency of the TMD is comprised in a relatively narrow band governed by the damping, and additional peaks appears around the natural frequency of the absorber. This feature leads to difficulties when the frequency of excitation or the natural frequency of the structure to be isolated is not known precisely. In recent studies, it has been demonstrated that various systems consisting of a Linear Oscillator (LO) and of a strong nonlinear attachment under transient loading are able to transfer irreversibly the energy from the LO to the NES [1, 2]. The dynamics which govern this Targeted Energy Transfer (TET) phenomenon is a $1:1$ resonance capture [3]. The transient energy pumping phenomenon has also been verified experimentally [4, 5].

Previous studies on TET motivate the interest to study the steady state energy pumping phenomenon [6–8]. It has been demonstrated that steady state response of the Nonlinear Energy Sink (NES) in the vicinity of the main resonance can exhibit quasiperiodic rather than periodic response [9]. Quasiperiodic response lead to energy exchange between the NES and the LO

which can be of practical interest for vibration mitigation. Experimental study of the response regime is the aim of this paper.

In the following section, the experimental setup is presented. The third section is devoted to the analytical treatment of the equation of motion. In the fourth section, experimental frequency response curves are presented, and comparison between experimental and analytical results are performed.

PRESENTATION OF THE EXPERIMENTAL SET-UP

The experimental fixture built to investigate the behavior of a single-degree-of-freedom oscillator strongly coupled to a nonlinear energy sink under periodic forcing is depicted in Fig. 1. It consists of a main mass (LO) grounded by means of a linear spring, and connected to an electrodynamic shaker. The nonlinear oscillator is embedded on this main mass. Both masses are connected by means of an essential cubic stiffness. All the slide guides are made with precision rail guides.

As shown in Fig. 1, the main system directly receive the electrodynamic force from the modal shaker. This force is constant whatever the response of the system is. Therefore, it has been considered as the input excitation force and the mass and stiffness of the shaker are considered with the LO. The exciter force is obtained by measuring the current delivered by the power amplifier.

The displacement of the two systems are measured using laser sensors. The stiffness nonlinearity has been implemented geometrically with two linear springs that extend axially and are free to rotate as shown in Fig. 2. The stiffness force - displacement relationship (given in Eqn. (1)), expressed in Taylor series expansion, is shown to be approximately cubic in nature, where u is the displacement, k_l is the linear spring stiffness, l the initial length of the spring, and P is the pre-stress force. Experimentally, P must be kept as small as possible, so the length of the springs attachment is tunable on the experiment.

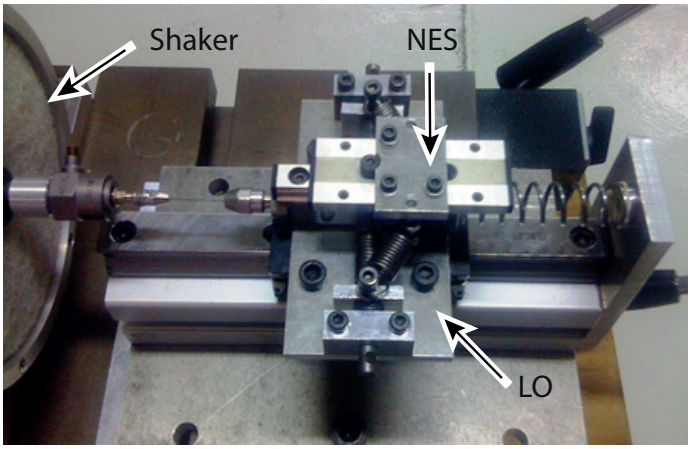

FIGURE 1: EXPERIMENTAL SET-UP

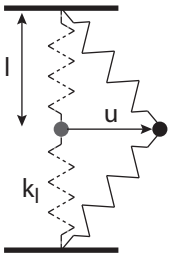

FIGURE 2: CUBIC RESTORING FORCE

$$f = 2k_l u + \frac{2u(P-k_l l)}{\sqrt{l^2+u^2}} \approx \frac{2P}{l}u + \frac{k_l - P}{l^3}u^3 + O\left(u^5\right) \qquad (1)$$

The experimental derived force displacement relationship is given in Fig. 3. The nonlinear stiffness value used in the theoretical analysis has been obtained with a nonlinear least square cubic polynomial fitting of the experimental curve.

TABLE 1: SYSTEM PARAMETERS

m_1	$0.761\,kg$	m_2	$0.098\,kg$
k_1	$5690\,N/m$	k_2	$1.473*10^6\,N/m^3$
c_1	$2.4\,Ns/m$	c_2	$0.1\,Ns/m$

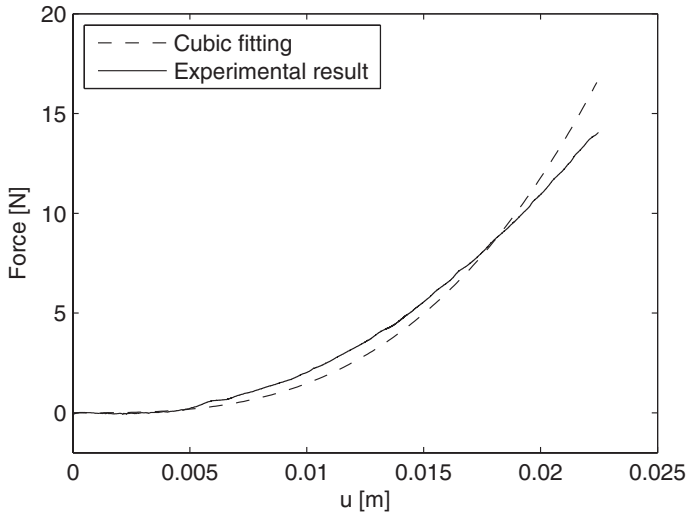

FIGURE 3: FORCE-DISPLACEMENT RELATIONSHIP

The parameters identified on the experimental setup and used for the calculations are given in Tab. 1. Hence, the aim of this fixture is to investigate the response of the linear oscillator and the NES for various forcing amplitude and frequency.

ANALYTICAL STUDY

In this section, the analytical study is developed. The main objective is to obtain theoretical response curve to explain the behavior observed on the experiments. Referring to the schema of the model (see Fig. 4), the general equations of motion are as follow:

$$\begin{aligned} m_1\ddot{x}+c_1\dot{x}+k_1x+c_2(\dot{x}-\dot{y})+k_2(x-y)^3 \\ = F\cos(\Omega t) \\ m_2\ddot{y}+c_2(\dot{y}-\dot{x})+k_2(y-x)^3=0 \end{aligned} \quad (2)$$

where x and y are the displacement of the linear oscillator and the attachment respectively, m_1 is the mass of the linear oscillator and the moving part of the electrodynamic shaker, m_2 is the mass of the nonlinear attachment, k_1 represent the sum of the of the linear spring stiffness, and the one of the electrodynamic shaker. c_1 and c_2 are the damping of the linear oscillator, and the nonlinear one, k_2 is the nonlinear spring stiffness, F and Ω are the forcing amplitude and frequency. The values of the system parameters are given in Tab. 1

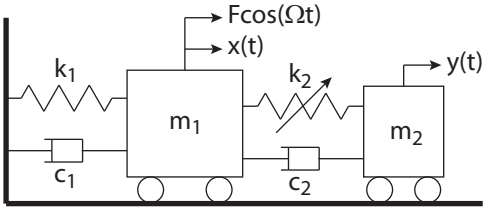

FIGURE 4: SCHEMA OF THE MODEL

Fixed points

Analytical treatment of the equations of motion follows the procedure proposed by Starosvetsky [10], based on the complexification averaging technique (CX-A) [11]. Introducing change of variables:

$$v=x+\varepsilon y \qquad w=x-y \quad (3)$$

reduces Eqn. (2) to the following form:

$$\begin{aligned} \ddot{v}+\frac{\varepsilon\lambda_1}{1+\varepsilon}\dot{v}+\frac{\varepsilon^2\lambda_1}{1+\varepsilon}\dot{w}+\frac{\omega_1^2}{1+\varepsilon}v+\frac{\varepsilon\omega_1^2}{1+\varepsilon}w=\varepsilon A\cos(\Omega t) \\ \ddot{w}+\frac{\varepsilon\lambda_1}{1+\varepsilon}\dot{v}+\frac{\varepsilon^2\lambda_1}{1+\varepsilon}\dot{w}+\frac{\omega_1^2}{1+\varepsilon}v+\frac{\varepsilon\omega_1^2}{1+\varepsilon}w+\lambda_2(1+\varepsilon)\dot{w} \\ +\omega_2^2(1+\varepsilon)w^3=\varepsilon A\cos(\Omega t) \end{aligned} \quad (4)$$

where $\varepsilon=\frac{m_2}{m_1}$, $\omega_1^2=\frac{k_1}{m_1}$, $\lambda_1=\frac{c_1}{m_2}$, $\lambda_2=\frac{c_2}{m_2}$, $\omega_2^2=\frac{k_2}{m_2}$, $A=\frac{F}{m_2}$. This change of variables physically corresponds to the consideration of the center of mass, and the relative displacement of the NES. The dynamic behavior is split into fast and slow varying component by introducing complex variable:

$$\phi_1 e^{i\Omega t}=\dot{v}+i\Omega v \qquad \phi_2 e^{i\Omega t}=\dot{w}+i\Omega w \quad (5)$$

where ϕ_1 represents the slow varying complex amplitude, and $\exp(i\Omega t)$ the fast varying component at the frequency of excitation. Introducing Eqn. (5) into Eqn. (4), and performing averaging procedure over one period of external excitation, yield the following slow modulated system:

$$\begin{aligned} \dot{\phi}_1+\frac{i\Omega\phi_1}{2}+\frac{\varepsilon\lambda_1\phi_1}{2(1+\varepsilon)}+\frac{\varepsilon^2\lambda_1\phi_2}{2(1+\varepsilon)}-\frac{i\omega_1^2\phi_1}{2\Omega(1+\varepsilon)} \\ -\frac{i\varepsilon\omega_1^2\phi_2}{2\Omega(1+\varepsilon)}-\frac{\varepsilon A}{2}=0 \\ \dot{\phi}_2+\frac{i\Omega\phi_2}{2}+\frac{\varepsilon\lambda_1\phi_1}{2(1+\varepsilon)}+\frac{\varepsilon^2\lambda_1\phi_2}{2(1+\varepsilon)}-\frac{i\omega_1^2\phi_1}{2\Omega(1+\varepsilon)} \\ -\frac{i\varepsilon\omega_1^2\phi_2}{2\Omega(1+\varepsilon)}+\frac{\lambda_2(1+\varepsilon)\phi_2}{2}-\frac{3i\omega_2^2(1+\varepsilon)|\phi_2|^2\phi_2}{8\Omega^3} \\ -\frac{\varepsilon A}{2}=0 \end{aligned} \quad (6)$$

Periodic solutions of system correspond to fixed points of Eqn. (6). These fixed points are found by setting the derivatives of Eqn. (6) to zero ($\dot{\phi}_1=\dot{\phi}_2=0$). By successive algebraic manipulations, their expressions can be reduced to the following form:

$$\phi_{1e}=\frac{-\frac{\varepsilon^2\lambda_1\phi_{2e}}{1+\varepsilon}+\frac{i\varepsilon\omega_1^2\phi_{2e}}{\Omega(1+\varepsilon)}+\varepsilon A}{i\Omega+\frac{\varepsilon\lambda_1}{1+\varepsilon}-\frac{i\omega_1^2}{\Omega(1+\varepsilon)}} \quad (7)$$

$$i\alpha_1|\phi_{2e}|^2\phi_{2e}+i\alpha_2\phi_{2e}+\alpha_3\phi_{2e}+\alpha_4+i\alpha_5 \quad (8)$$

where ϕ_{1e} and ϕ_{2e} stand for the fixed poind and α_i ($i=1..5$) are real coefficients given in appendix A. Expressing ϕ_{2e} in polar

form $\phi_{2e} = |\phi_{2e}|e^{i\theta_2}$, yield to the following polynomial which roots correspond to the fixed points of Eqn. (6):

$$\alpha_1^2\Phi_2^3 + 2\alpha_1\alpha_2\Phi_2^2 + (\alpha_2^2+\alpha_3^2)\Phi_2 = \alpha_4^2+\alpha_5^2 \tag{9}$$

with $\Phi_2 = |\phi_{2e}|^2$. This system is solved analytically, and the fixed points are computed for varying frequency, then the steady state response of the two oscillators are obtained by reversing changes of variable:

$$w(t) = \frac{|\phi_2|}{\Omega}\sin(\Omega t+\theta_2) \tag{10}$$

$$x(t) = \frac{\sqrt{\Phi_1+\varepsilon^2\Phi_2+2\varepsilon|\phi_1\phi_2|}}{\Omega(1+\varepsilon)} sin\left(\Omega t + atan\left(\frac{|\phi_1|sin(\theta_1)+\varepsilon|\phi_2|sin(\theta_2)}{|\phi_1|cos(\theta_1)+\varepsilon|\phi_2|cos(\theta_2)}\right)\right) \tag{11}$$

Since large relative response w signifies resonance interaction of the NES and the LO which is one of the condition for enhancing TET. This relative displacement of the NES (w) is kept in what follows.

Stability of fixed points

In this part, the stability of the periodic solutions of Eqn. (6) is investigated. To this end, small complex perturbations of the fixed points are introduced:

$$\phi_1 = \phi_{1e}+\delta_1 \qquad \phi_2 = \phi_{2e}+\delta_2 \tag{12}$$

Substituting (12) into (6) and linearizing around the small perturbation yield the following system of ODEs:

$$\dot{\delta}_1 = \left(\frac{i\omega_1^2}{2\Omega(1+\varepsilon)} - \frac{\varepsilon\lambda_1}{2(1+\varepsilon)} - \frac{i\Omega}{2}\right)\delta_1 + \left(\frac{i\varepsilon\omega_1^2}{2\Omega(1+\varepsilon)} - \frac{\varepsilon^2\lambda_1}{2(1+\varepsilon)}\right)\delta_2$$

$$\dot{\delta}_1^* = \left(-\frac{i\omega_1^2}{2\Omega(1+\varepsilon)} - \frac{\varepsilon\lambda_1}{2(1+\varepsilon)} + \frac{i\Omega}{2}\right)\delta_1^* + \left(-\frac{i\varepsilon\omega_1^2}{2\Omega(1+\varepsilon)} - \frac{\varepsilon^2\lambda_1}{2(1+\varepsilon)}\right)\delta_2^*$$

$$\dot{\delta}_2 = \left(\frac{i\omega_1^2}{2\Omega(1+\varepsilon)} - \frac{\varepsilon\lambda_1}{2(1+\varepsilon)}\right)\delta_1 + \left(\frac{3i\omega_2^2(1+\varepsilon)\Phi_2}{4\Omega^3} + \frac{i\varepsilon\omega_1^2}{2\Omega(1+\varepsilon)} - \frac{\varepsilon^2\lambda_1}{2(1+\varepsilon)} - \frac{\lambda_2(1+\varepsilon)}{2} - \frac{i\Omega}{2}\right)\delta_2 + \frac{3i\omega_2^2(1+\varepsilon)\phi_2^2}{8\Omega^3}\bar{\delta}_2$$

$$\dot{\delta}_2^* = \left(-\frac{i\omega_1^2}{2\Omega(1+\varepsilon)} - \frac{\varepsilon\lambda_1}{2(1+\varepsilon)}\right)\delta_1^* + \left(-\frac{3i\omega_2^2(1+\varepsilon)\Phi_2^*}{4\Omega^3} - \frac{i\varepsilon\omega_1^2}{2\Omega(1+\varepsilon)} - \frac{\varepsilon^2\lambda_1}{2(1+\varepsilon)} - \frac{\lambda_2(1+\varepsilon)}{2} + \frac{i\Omega}{2}\right)\delta_2^* - \frac{3i\omega_2^2(1+\varepsilon)\phi_2^{*2}}{8\Omega^3}\delta_2 \tag{13}$$

Writing system of Eqn. (13) into matricial form, the stability of the fixed poind is directly derived from the eigenvalues of this matrix. If all eigenvalues have a negative real part, the fixed point is stable. In the opposite, if only one of these eigenvalues has a positive real part, the fixed point is denoted as unstable. In addition, if a fixed point possesses a pair of pure imaginary eigenvalues, it follows a generic Hopf bifurcation in the slow flow, which yield to quasiperiodic motion.

Figure 5 shows a comparison between the slow modulated amplitude of the relative displacement of the NES obtained using the CX-A technique, and the one obtained by step by step integration of the equation of motion (2). The point a (see Fig. 6) choosed in a stable predicted region which is confirmed by numerical integration. On the contrary, the point b choosed after the Hopf bifurcation of the main branch clearly shown quasiperiodic oscillation.

EXPERIMENTAL RESULT AND COMPARISON

The aim of the experimental tests is to obtain the nonlinear frequency response function of the system around the $1:1$ resonance. To this end, the displacement signals of both the LO and the NES have been recorded for increasing and decreasing frequency varying from $5Hz$ to $20Hz$ by step of $0.5Hz$. Time measurement data are then exported to MATLAB for post-processing. Two excitations levels are considered herein corresponding to forcing amplitudes of 2.7 and $2.0N$. The Root Mean Square (RMS) value of the absolute displacement of the LO (x) and the relative displacement between the NES and the LO (w) are plotted versus the frequency of excitation.

Figures 6 and 7 show the nonlinear response curves for the NES and the LO respectively, for a forcing amplitude of $2.7N$. Thin lines correspond to stable periodic motion, and bold lines

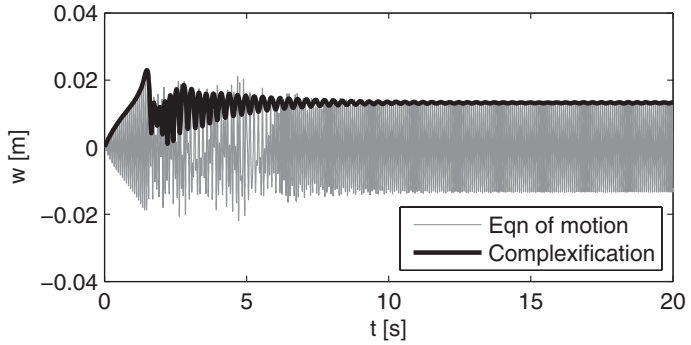

(a) Stable periodic motion at $13.9\,Hz$

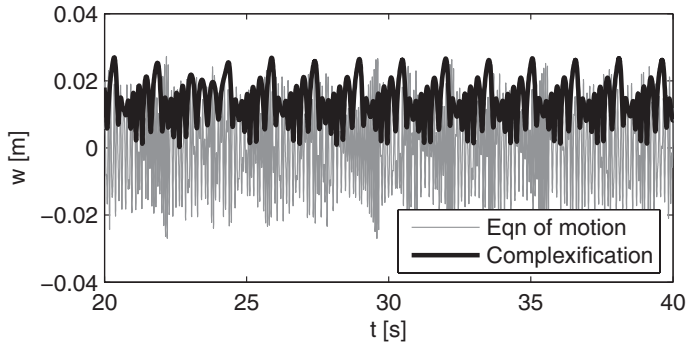

(b) Stable quasiperiodic motion at $14.3\,Hz$

FIGURE 5: COMPARISON OF THE RELATIVE DISPLACEMENT OF THE NES BETWEEN COMPLEXIFICATION AN NUMERICAL INTEGRATION ($F = 2.7N$, $f = 14.5\,Hz$)

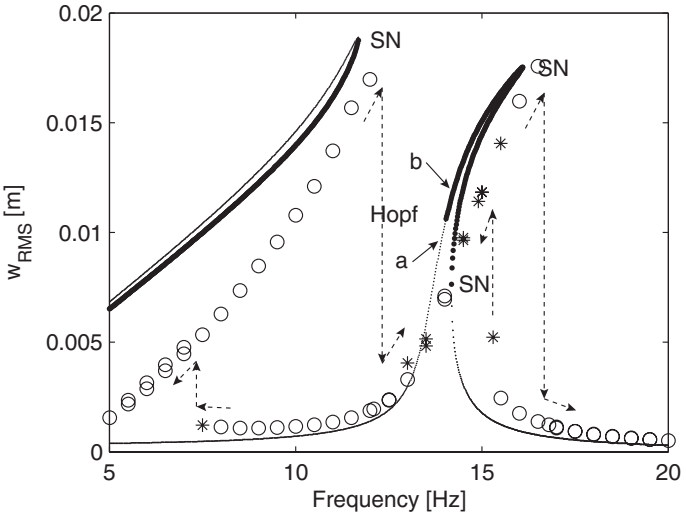

FIGURE 6: EXPERIMENTAL AND ANALYTICAL *NES* FREQUENCY RESPONSE ($F = 2.7N$) ("o": experimental periodic oscillation, "$*$": experimental modulated oscillation, thin line: analytical stable fixed points, thick line: analytical unstable fixed point)

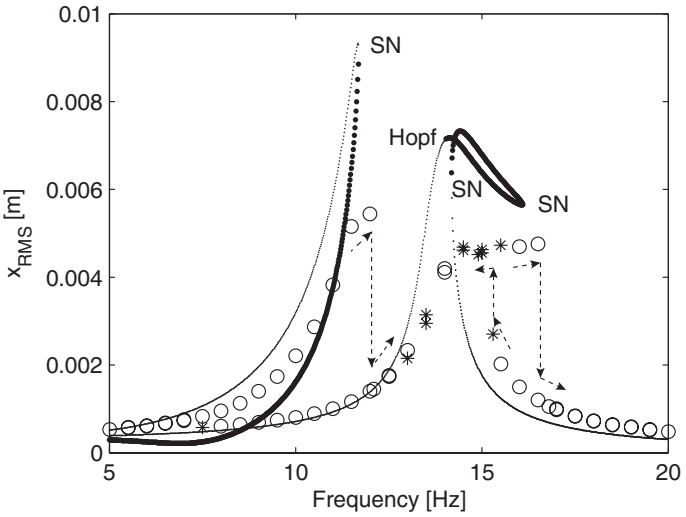

FIGURE 7: EXPERIMENTAL AND ANALYTICAL *LO* FREQUENCY RESPONSE ($F = 2.7N$) ("o": experimental periodic oscillation, "$*$": experimental modulated oscillation, thin line: analytical stable fixed points, thick line: analytical unstable fixed point)

refer to unstable region of periodic solutions. The bifurcation points and their type are indicated on the diagrams. In addition to the classical resonance curve, a secondary resonance curve with a stable upper branch is observed.

Those figures also display the measured frequency response of both oscillators, where "o" and "$*$" denote periodic and quasiperiodic regimes respectively, and arrows show the jumps, and the direction of evolution of the frequency. It can be noticed that experimental and analytical response curves are shown to be in good agreement. At the beginning ($5\,Hz$), when the frequency is increasing, the motion take place on the stable upper branch before jumping on the lower branch at $12.5\,Hz$. Then, amplitude of motion increases again when following the main resonance curve. At this time, quasiperiodic regime takes place as it can be seen in Fig. 8. This clearly shows a modulated response which match well with a Hopf bifurcation. However, unlike the prediction obtained with the CX-A technique, motion of the oscillators becomes again periodic before jumping back on the lower curve. Nevertheless, the frequency at which the jump occurs is approximately the same in the both case.

When the forcing amplitude is reduced (see Figs 9, 10) to $2.0N$, it implies some changes in the behavior of the system. On the theoretical response, no more Hopf and Saddle Node (SN) bifurcation occurs, and the main branch at the natural frequency

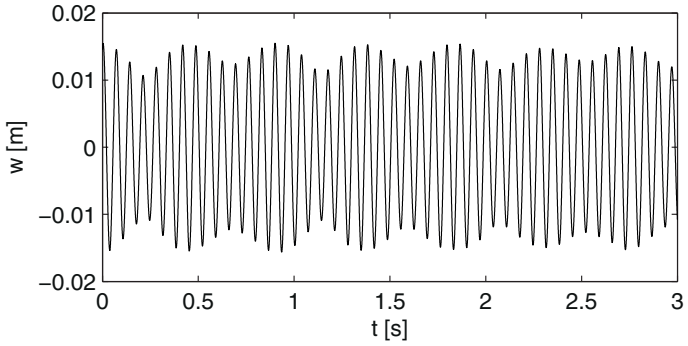

FIGURE 8: TIME MEASUREMENT OF QUASIPERIODIC RESPONSE ($F = 2.7N$ $f = 14.5Hz$)

of the LO tends to be linear. These predictions are however not confirmed by the experiments which still shown a narrow zone of quasiperiodic response. These discrepancies are explained by a minor difference in the identification of the damping, or in the identification of the nonlinear stiffness. These parameters are difficult to identify precisely, and numerical simulation have shown that even a small changes of these parameters induce qualitative different behavior.

Comparing experimental and theoretical results, it is interesting to notice that there is qualitative agreement even if differences occurs on the amplitude, and instability zones. There are

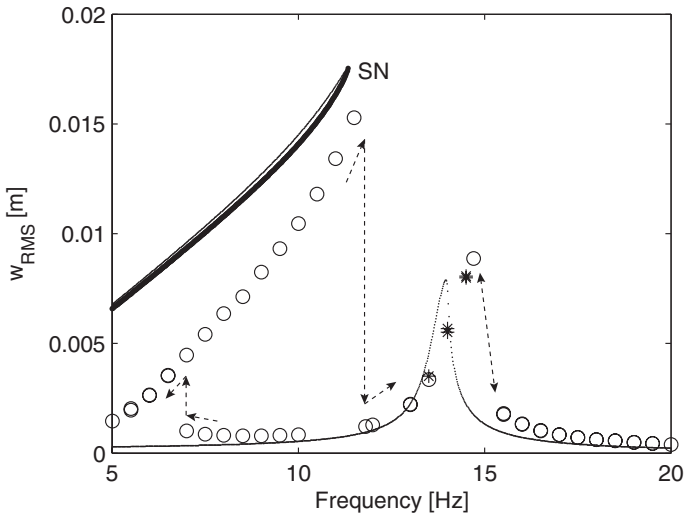

FIGURE 9: EXPERIMENTAL AND ANALYTICAL *NES* FREQUENCY RESPONSE ($F = 2.0N$) ("o": experimental periodic oscillation, "$*$": experimental modulated oscillation, thin line: analytical stable fixed points, thick line: analytical unstable fixed point)

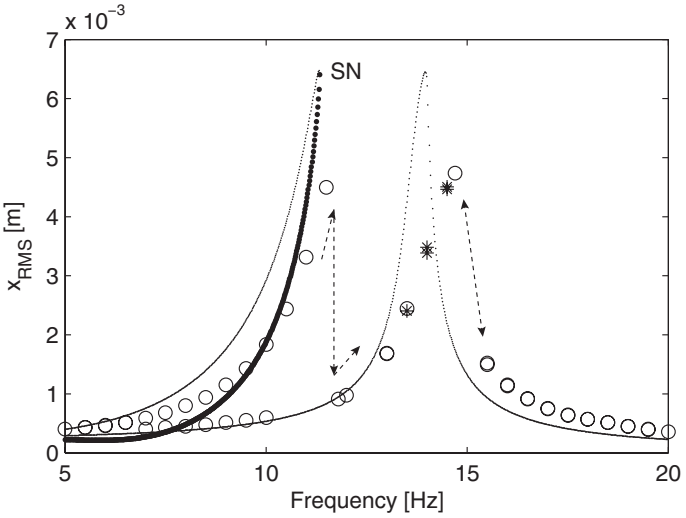

FIGURE 10: EXPERIMENTAL AND ANALYTICAL *LO* FREQUENCY RESPONSE ($F = 2.0N$) ("o": experimental periodic oscillation, "$*$": experimental modulated oscillation, thin line: analytical stable fixed points, thick line: analytical unstable fixed point)

mainly attributed to the uncertainty on the characterization of the nonlinear stiffness, and damping.

CONCLUDING REMARKS

The purpose of this study was the experimental and theoretical investigations of the response regimes of a linear oscillator coupled to a NES around the 1 : 1 resonance. This seemingly simple system has exhibited a highly complicated dynamic behavior. At low forcing amplitude, the system frequency response curve still has shown two branches, but the main one is almost linear. However, when the excitation level was increased, the system has exhibited periodic and also modulated response. These modulated responses are of big interest, since they are synonym of energy exchange between the NES and the LO. The behavior of the system has been explained using the CX-A technique, however there was some discrepancies, mainly attributed to parameters identification problem (damping, nonlinear stiffness). The use of other methods such as multiple scale analysis might be useful to explain the modulated regimes more precisely. Others regimes have been observed in the experimental setup, such as internal resonance.

REFERENCES

[1] Gourdon, E., Alexander, N., Taylor, C., Lamarque, C., and Pernot, S., 2007. "Nonlinear energy pumping under transient forcing with strongly nonlinear coupling: Theoretical

and experimental results". *Journal of Sound and Vibration,* ***300***(3-5), pp. 522 – 551.

[2] Kerschen, G., Lee, Y. S., Vakakis, A. F., McFarland, D. M., and Bergman, L. A., 2005. "Irreversible passive energy transfer in coupled oscillators with essential nonlinearity". *SIAM Journal on Applied Mathematics,* ***66***(2), pp. 648–679.

[3] Gendelman, O., Manevitch, L. I., Vakakis, A. F., and M'Closkey, R., 2001. "Energy pumping in nonlinear mechanical oscillators: Part i—dynamics of the underlying hamiltonian systems". *Journal of Applied Mechanics,* ***68***(1), pp. 34–41.

[4] Gourdon, E., Alexander, N., Taylor, C., Lamarque, C., and Pernot, S., 2007. "Nonlinear energy pumping under transient forcing with strongly nonlinear coupling: Theoretical and experimental results". *Journal of Sound and Vibration,* ***300***(3-5), pp. 522 – 551.

[5] McFarland, D. M., Bergman, L. A., and Vakakis, A. F., 2005. "Experimental study of non-linear energy pumping occurring at a single fast frequency". *International Journal of Non-Linear Mechanics,* ***40***(6), pp. 891 – 899.

[6] Berlioz, A., Dufour, R., and Sinha, S. C., 2000. "Bifurcation in a nonlinear autoparametric system using experimental and numerical investigations". *Nonlinear Dynamics,* ***23***, pp. 175–187.

[7] Alexander, N. A., and Schilder, F., 2009. "Exploring the performance of a nonlinear tuned mass damper". *Journal of Sound and Vibration,* ***319***(1-2), pp. 445 – 462.

[8] Jiang, X., McFarland, D. M., Bergman, L. A., and Vakakis, A. F., 2003. "Steady state passive nonlinear energy pumping in coupled oscillators: Theoretical and experimental results". *Nonlinear Dynamics,* ***33***, pp. 87–102.

[9] Gendelman, O., Gourdon, E., and Lamarque, C., 2006. "Quasiperiodic energy pumping in coupled oscillators under periodic forcing". *Journal of Sound and Vibration,* ***294***(4-5), pp. 651 – 662.

[10] Starosvetsky, Y., and Gendelman, O., 2008. "Response regimes of linear oscillator coupled to nonlinear energy sink with harmonic forcing and frequency detuning". *Journal of Sound and Vibration,* ***315***(3), pp. 746 – 765.

[11] Manevitch, L. I., 2001. "The description of localized normal modes in a chain of nonlinear coupled oscillators using complex variables". *Nonlinear Dynamics,* ***25***, pp. 95–109.

Appendix A: Coefficients of Eqn. (8)

$$\alpha_1 = -\frac{3i\omega_2^2(1+\varepsilon)}{8\Omega^3} \tag{14}$$

$$\alpha_2 = \left[\frac{\omega_1^2\varepsilon^3\lambda_1^2}{\Omega(1+\varepsilon)} - \frac{\omega_1^4\varepsilon}{\Omega^2}\left(\frac{\Omega}{2} - \frac{\omega_1^2}{2\Omega(1+\varepsilon)}\right) + \varepsilon^3\lambda_1^2\left(\frac{\Omega}{2} - \frac{\omega_1^2}{2\Omega(1+\varepsilon)}\right)\right]\left[4(1+\varepsilon)^2\left(\frac{\varepsilon^2\lambda_1^2}{4(1+\varepsilon)^2} + \left(\frac{\Omega}{2} - \frac{\omega_1^2}{2\Omega(1+\varepsilon)}\right)^2\right)\right]^{-1} + \frac{\Omega}{2} - \frac{\varepsilon\omega_1^2}{2\Omega(1+\varepsilon)} \tag{15}$$

$$\alpha_3 = \left[\frac{\omega_1^4\varepsilon^3\lambda_1}{4\Omega^2(1+\varepsilon)} + \frac{\omega_1^2\varepsilon^2\lambda_1}{\Omega}\left(\frac{\Omega}{2} - \frac{\omega_1^2}{2\Omega(1+\varepsilon)}\right) - \frac{\varepsilon^4\lambda_1^3}{4}\right]\left[2(1+\varepsilon)^2\left(\frac{\varepsilon^2\lambda_1^2}{4(1+\varepsilon)^2} + \left(\frac{\Omega}{2} - \frac{\omega_1^2}{2\Omega(1+\varepsilon)}\right)^2\right)\right]^{-1} + \frac{\varepsilon^2\lambda_1}{2(1+\varepsilon)} + \frac{\lambda_2(1+\varepsilon)}{2} \tag{16}$$

$$\alpha_4 = \left[\frac{\varepsilon^3\lambda_1^2 A}{2(1+\varepsilon)} - \frac{\varepsilon\omega_1^2 A}{\Omega}\left(\frac{\Omega}{2} - \frac{\omega_1^2}{2\Omega(1+\varepsilon)}\right)\right] \times \left[4(1+\varepsilon)\left(\frac{\varepsilon^2\lambda_1^2}{4(1+\varepsilon)^2} + \left(\frac{\Omega}{2} - \frac{\omega_1^2}{2\Omega(1+\varepsilon)}\right)^2\right)\right]^{-1} - \frac{\varepsilon A}{2} \tag{17}$$

$$\alpha_5 = \left[-\frac{\varepsilon^2\omega_1^2\lambda_1 A}{2\Omega(1+\varepsilon)} - \frac{\varepsilon^2\lambda_1 A}{\Omega}\left(\frac{\Omega}{2} - \frac{\omega_1^2}{2\Omega(1+\varepsilon)}\right)\right] \times \left[4(1+\varepsilon)\left(\frac{\varepsilon^2\lambda_1^2}{4(1+\varepsilon)^2} + \left(\frac{\Omega}{2} - \frac{\omega_1^2}{2\Omega(1+\varepsilon)}\right)^2\right)\right]^{-1} \tag{18}$$